

Simplex Representation for Subspace Clustering

Jun Xu¹, *Student Member, IEEE*, Deyu Meng², *Member, IEEE*, Lei Zhang¹, *Fellow, IEEE*

¹Department of Computing, The Hong Kong Polytechnic University, Hong Kong SAR, China

²School of Mathematics and Statistics, Xi'an Jiaotong University, Xi'an, China

Spectral clustering based methods have achieved leading performance on subspace clustering problem. State-of-the-art subspace clustering methods follow a three-stage framework: compute a coefficient matrix from the data by solving an optimization problem; construct an affinity matrix from the coefficient matrix; and obtain the final segmentation by applying spectral clustering to the affinity matrix. To construct a feasible affinity matrix, these methods mostly employ the operations of exponentiation, absolutely symmetrization, or squaring, etc. However, all these operations will force the negative entries (which cannot be explicitly avoided) in the coefficient matrix to be positive in computing the affinity matrix, and consequently damage the inherent correlations among the data. In this paper, we introduce the simplex representation (SR) to remedy this problem of representation based subspace clustering. We propose an SR based least square regression (SRLSR) model to construct a physically more meaningful affinity matrix by integrating the nonnegative property of graph into the representation coefficient computation while maintaining the discrimination of original data. The SRLSR model is reformulated as a linear equality-constrained problem, which is solved efficiently under the alternating direction method of multipliers framework. Experiments on benchmark datasets demonstrate that the proposed SRLSR algorithm is very efficient and outperforms state-of-the-art subspace clustering methods on accuracy.

Index Terms—Subspace clustering, simplex representation, spectral clustering.

I. INTRODUCTION

HIGH-dimensional data are commonly observed in various computer vision and image processing problems. Contrary to their high-dimensional appearance, the latent structure of those data usually lie in a union of low-dimensional subspaces [1]. Recovering the latent low-dimensional subspaces from the high-dimensional observation can not only reduce the computational cost and memory requirements of subsequent algorithms, but also reduce the noise corrupted in the high-dimensional data. In many machine learning and computer vision tasks, we need to find the clusters of high-dimensional data such that each cluster can be fitted by a subspace, which is referred to as the subspace clustering (SC) problem [1].

SC has been extensively studied in the past decades [2]–[33]. Most of existing SC methods can be categorized into four categories: iterative based methods [2], [3], algebraic based methods [4]–[6], statistical based methods [7]–[10], and spectral clustering based methods [14]–[33]. Among these four categories, spectral clustering based methods have become the mainstream due to their theoretical guarantees and promising performance on real-world applications such as motion segmentation [16] and face clustering [18]. The spectral clustering based methods usually follow a three-step framework: **Step 1**) obtain a coefficient matrix of the data points by solving an optimization problem, which usually incorporates sparse or low rank regularizations due to their good mathematical properties; **Step 2**) construct an affinity matrix from the coefficient matrix by employing exponentiation [14], absolutely symmetrization [15], [16], [20], [23]–[31], and squaring operations [17]–[19], [32], [33], etc.; **Step 3**) apply spectral analysis techniques [34] to the affinity matrix and obtain the final clusters of the data points.

Most spectral clustering based methods [14]–[33] obtain the expected coefficient matrix under the *self-expressiveness*

property [15], [16], which states that each data point in a union of multiple subspaces can be *linearly* represented by the other data points in the same subspace. However, in some real-world applications, the data points lie in a union of multiple affine subspaces rather than linear subspaces [16]. A trivial solution is to ignore the affine structure of the data points and directly perform clustering as in the subspaces of linear structures. A non-negligible drawback of this solution is the increasing dimension of the intersection of two subspaces, which can make the subspaces indistinguishable from each other [16]. To cluster data points lying in affine subspaces instead of linear subspaces, the affine constraint is introduced [15], [16], in which each data point can be written as an affine combination of other points with the sum of coefficients being one.

Despite their high clustering accuracy, most of spectral clustering based methods [14]–[33] suffer from three major drawbacks. First, under the affine constraint, the coefficient vector is not flexible enough to handle real-world applications where the data points are corrupted by noise or outliers. Second, negative coefficients cannot be fully avoided since the existing methods do not explicitly consider non-negative constraint in **Step 1**. However, in real-world applications, it is physically problematic to reconstruct a data point by allowing the others to “cancel each other out” with complex additions and subtractions [35]. Thus, most of these methods are limited by being stranded at this physical bottleneck. Third, the exponentiation, absolutely symmetrization, and squaring operations in **Step 2** will force the negative coefficients to be positive ones, and thus damage the inherent correlations among the data points.

To solve the three drawbacks mentioned above, we introduce the Simplex Representation (SR) for spectral clustering based SC. Specifically, the SR is introduced from two interdependent aspects. First, to broaden its adaptivity to real scenarios, we extend the affine constraint to the scaled affine constraint, in which the coefficient vector in the optimization

model will sum up to a scalar s ($s > 0$) instead of 1. By changing the value of s , we can adapt the generative and discriminative properties of the optimization model. Note that the affine constraint is only a special case of the introduced scaled affine constraint when $s = 1$. Second, to make the overall optimization model physically more meaningful, we introduce the non-negative constraint on the coefficients in the optimization model. The introduction of non-negative constraint have at least three benefits: 1) in **Step 1**, it can avoid complex additions and subtractions among the data points in the optimization model; 2) since the coefficient matrix is naturally non-negative in **Step 1**, it maintains the inherent correlations among the data points by avoiding the operations of exponentiation, absolutely symmetrization, and squaring for building the affinity matrix in **Step 2**; 3) with the scaled affine constraint, the non-negativity can enhance the discriminativity of the coefficients, so that the input data point will more likely be reconstructed by the data points from the same subspace. With the introduced SR, a novel SC model called SR based Least Square Regression (SRLSR) is proposed. Our experiments on commonly used benchmark datasets show that the proposed SRLSR is very efficient and it achieves lower clustering errors than state-of-the-art SC algorithms.

The major contributions of this article are summarized as follows:

- We introduce a new representation framework, i.e., the Simplex Representation (SR), as an alternative to the popular sparse or low rank representation to solve the SC problem. The proposed SR can maintain the inherent correlations among the data points, and thus remedy the damages on the affinity matrix brought by previous spectral clustering based SC methods. As far as we know, our work is among the first to introduce SR to solve the SC problem.
- We propose an SRLSR model to solve the SC problem. We reformulate the proposed SRLSR model into a linear equality-constrained problem with two variables, and solve the relaxed problem with an alternating direction method of multipliers [36] algorithm. Each variable can be updated efficiently, and the convergence of the algorithm can be guaranteed.
- Experiments on three benchmark datasets, i.e., the Hopkins 155 dataset [37], the Extended Yale B dataset [38], and the MNIST dataset [39], demonstrate that the proposed SRLSR algorithm is very efficient, and it achieves much better performance than state-of-the-art SC algorithms on motion segmentation, face clustering, and digit clustering. The code will be released with the publication of this paper.

The remainder of this paper is organized as follows. Section II provides a brief survey of related work. In section III, we first present the proposed SRLSR model, and then provide the optimization of the SRLSR model, and finally give an SRLSR based SC algorithm. In Section IV, extensive experiments are conducted to evaluate the SRLSR algorithm and compare it with state-of-the-art SC algorithms. Finally, several concluding remarks are given in Section V.

II. RELATED WORK

A. Prior Work on Subspace Clustering

Over the past decades, numerous subspace clustering (SC) algorithms [2]–[33] have been proposed. According to the mathematical frameworks they employ, most of existing SC algorithms can be divided into four main categories: iterative methods, algebraic methods, statistical methods, and spectral clustering based methods.

The iterative methods such as K-subspaces [2] and algebraic subspace clustering (ASC) [3] solve the SC problem by alternating between assigning points to subspaces and fitting subspaces to corresponding clusters. Such approaches are limited by the requirement to know the number and dimensions of the subspaces, and they are sensitive to the initialization.

The algebraic methods solve the SC problem by modeling each subspace as a gradient of a polynomial [4]–[6]. These methods do not require prior information of each subspace, and can enforce structural restriction on the subspaces. Two representative methods in this category are the Shape Interaction Matrix (SIM) [4] and the Generalized Principal Component Analysis (GPCA) [5]. The algebraic methods suffer from exponentially expensive computations due to the polynomial fitting. Besides, these methods are sensitive to noise and outliers, and thus difficult to cluster points near the intersection of subspaces.

The statistical methods model each subspace as a Gaussian distribution, and solve the SC problem as an estimation of mixture of Gaussians. Specific algorithms include Agglomerative Lossy Compression (ALC) [10], Mixture of Probabilistic PCA (MPPCA) [7], Multi-Stage Learning (MSL) [8], and the well-known RANSAC [9]. These methods typically require prior information of the latent subspaces, such as the number of subspaces and their dimensions. The computational complexity of these methods is also exponential with respect to the number of subspaces and their dimensions.

The spectral clustering methods use local information around each data point to compare the similarity between a pair of points. The clustering of data points is achieved by applying spectral clustering to the affinity matrix. Local Subspace Affinity (LSA) [11], Spectral Local Best-fit Flats (SLBF) [12], Locally Linear Manifold Clustering (LLMC) [13], and Spectral Curvature Clustering (SCC) [14] are methods of this class. However, they can not deal well with points near the intersection of two subspaces if the neighborhood of one point contains points from different subspaces. Inspired by the work of compressed sensing [40], [41], the Sparse Subspace Clustering (SSC) algorithm [15], [16] solves the clustering problem by seeking a sparse representation of data points over a dictionary. By resolving the sparse representations for all data points and constructing an affinity graph, SSC automatically finds different subspaces as well as their dimensions from a union of subspaces. Finally, the SC is performed by spectral clustering [42]. A robust version of SSC to deal with noise and corruptions or missing observations is also given in [15], [16].

Instead of finding a sparse representation, the Low-Rank Representation (LRR) method [17]–[19] poses the SC problem

as finding a low-rank representation of the data over the data itself. Lu *et al.* proposed a clustering method based on Least Squares Regression (LSR) [23] to take advantage of data correlation and group highly correlated data together. The grouping information can be used to construct an affinity matrix which is block diagonal and can be used for SC through spectral clustering algorithms. Recently, Lin *et al.* analyzed the grouping effect deeply and proposed a SMOOTH Representation framework [24] which also achieves state-of-the-art performance in subspace clustering problem. Different from SSC, the LRR, LSR, and SMR algorithms all use Normalized Cuts [43] in the spectral clustering step. You *et al.* proposed a scalable SSC method to solve the SSC model [16] via Orthogonal Matching Pursuit [31].

B. The Spectral Clustering based Framework

Most of state-of-the-art SC methods are designed under the spectral clustering framework. Mathematically, denote by $\mathbf{X} = [\mathbf{x}_1, \dots, \mathbf{x}_N] \in \mathbb{R}^{D \times N}$ the data matrix, each data point $\mathbf{x}_i \in \mathbb{R}^D$, $i \in \{1, \dots, N\}$, in \mathbf{X} can be expressed as

$$\mathbf{x}_i = \mathbf{X} \mathbf{c}_i, \quad (1)$$

where $\mathbf{c}_i \in \mathbb{R}^N$ is the coefficient vector. One can also put the data points column by column and rewrite (1) as

$$\mathbf{X} = \mathbf{X} \mathbf{C}, \quad (2)$$

where $\mathbf{C} \in \mathbb{R}^{N \times N}$ is the coefficient matrix. To find the desired \mathbf{C} , existing SC methods [15]–[18], [20], [23]–[32] impose on \mathbf{C} different regularizations such as sparsity and low rankness. Denote by $\|\cdot\|_F$, $\|\cdot\|_1$, $\|\cdot\|_2$, $\|\cdot\|_{2,1}$, $\|\cdot\|_*$, λ , and p the Frobenius norm, the ℓ_1 norm, the ℓ_2 norm, the $\ell_{2,1}$ norm, the nuclear norm, the regularization parameter, and a positive integer, respectively. The optimization models of some representative work are summarized as follows:

Sparse Subspace Clustering (SSC) [16]:

$$\min_{\mathbf{C}} \|\mathbf{C}\|_1 \quad \text{s.t.} \quad \mathbf{X} = \mathbf{X} \mathbf{C}, \mathbf{1}^\top \mathbf{C} = \mathbf{1}^\top, \text{diag}(\mathbf{C}) = \mathbf{0}. \quad (3)$$

Low-Rank Representation (LRR) [18]:

$$\min_{\mathbf{C}} \|\mathbf{X} - \mathbf{X} \mathbf{C}\|_{2,1} + \lambda \|\mathbf{C}\|_*. \quad (4)$$

Least Squares Regression (LSR) [23]:

$$\min_{\mathbf{C}} \|\mathbf{X} - \mathbf{X} \mathbf{C}\|_F^2 + \lambda \|\mathbf{C}\|_F^2 \quad \text{s.t.} \quad \text{diag}(\mathbf{C}) = \mathbf{0}. \quad (5)$$

SSC by Orthogonal Matching Pursuit (SSCOMP) [31]:

$$\min_{\mathbf{c}_i} \|\mathbf{x}_i - \mathbf{X} \mathbf{c}_i\|_2^2 \quad \text{s.t.} \quad \|\mathbf{c}_i\|_0 \leq p, c_{ii} = 0. \quad (6)$$

Once the coefficient matrix \mathbf{C} is computed, the affinity matrix \mathbf{A} is usually constructed by exponentiation [14], absolutely symmetrization [15], [16], [20], [23]–[31], and squaring operation [17], [18], [32], etc. For example, the widely used absolutely symmetrization operation in [15], [16], [20], [23]–[31] is defined by

$$\mathbf{A} = \frac{|\mathbf{C}| + |\mathbf{C}^\top|}{2}. \quad (7)$$

After the affinity matrix \mathbf{A} is obtained, spectral clustering techniques [43] are applied on it to obtain the final segmentation of the subspaces.

However, the spectral clustering framework suffers from one major bottleneck: the exponentiation, absolutely symmetrization, and squaring operations will force the negative entries in \mathbf{C} to be positive in \mathbf{A} , and hence damage the inherent correlations among the data points in \mathbf{X} . Besides, the affine constraint in SSC limits the model flexibility, making SSC difficult to deal with complex real world applications. In order to remedy these drawbacks, in this paper, we introduce the simplex representation into the SC problem.

III. SIMPLEX REPRESENTATION BASED SUBSPACE CLUSTERING

In this section, we propose a Simplex Representation (SR) based Least Square Regression (SRLSR) model, develop an optimization algorithm to solve it, and present a novel SRLSR based algorithm for SC.

A. The SRLSR Model

Given a set of data points $\mathcal{X} = \{\mathbf{x}_i \in \mathbb{R}^D\}_{i=1}^N$ drawn from a union of n subspaces $\{\mathcal{S}_j\}_{j=1}^n$, SC aims to cluster the data points in \mathcal{X} into n groups in which each group only contains the data points from the same subspace. To this end, we propose an SR based model

$$\min_{\mathbf{c}_i} \|\mathbf{x}_i - \mathbf{X} \mathbf{c}_i\|_2^2 + \lambda \|\mathbf{c}_i\|_2^2 \quad \text{s.t.} \quad \mathbf{c}_i \geq 0, \mathbf{1}^\top \mathbf{c}_i = s, \quad (8)$$

where \mathbf{c}_i is the coefficient vector of \mathbf{x}_i over the data matrix \mathbf{X} , and $\mathbf{c}_i \geq 0$ means that each entry of \mathbf{c}_i is non-negative. $\mathbf{1}$ is the vector of all ones and $s > 0$ is a scalar denoting the sum of entries in the coefficient vector \mathbf{c}_i . We use the term “simplex” here because the entries in the coefficient vector \mathbf{c}_i are constrained by a positive simplex, i.e., non-negative and sum up to a scalar s .

In real-world applications, data are often corrupted by outliers due to ad-hoc data collection techniques. Existing SC methods deal with outliers by explicitly modeling them as an additional variable, and updating this variable using the ADMM algorithm. For example, in the seminal work of SSC [15], [16] and its successors [23], [25], [28], [30], c_{ii} is set as 0 for \mathbf{x}_i , indicating that each data point cannot be represented by itself, thus avoiding trivial solution of identity matrix. However, this will bring more computational cost and make the whole algorithm hardly convergent [16], [18].

Different from these existing methods [16], [23], [25], [28], [30], we do not consider the constraint of $c_{ii} = 0$ for three major reasons. 1) First, the regularization term with positive λ can naturally avoid the potential trivial solution of identity matrix $\mathbf{C} = \mathbf{I}$. 2) Second, allowing $c_{ii} \neq 0$ has a clear physical meaning that it can allow a sample \mathbf{x}_i in the subspace to be *partially* represented by itself. This is particularly useful when \mathbf{x}_i is corrupted by noise. 3) Third, when the data are corrupted by outliers in the same subspace, $c_{ii} = 1$ can help each data point \mathbf{x}_i *fully* represents itself. By removing the constraint of $c_{ii} = 0$, our proposed SRLSR model is very robust to

noise and outliers, as will be demonstrated in the experimental section (Section IV).

We can also rewrite the SR based model (8) for all N data points into the matrix form and obtain

$$\begin{aligned} \min_C & \|X - XC\|_F^2 + \lambda \|C\|_F^2 \\ \text{s.t. } & C \geq 0, \mathbf{1}^\top C = s\mathbf{1}^\top, \end{aligned} \quad (9)$$

where $C \in \mathbb{R}^{N \times N}$ is the coefficient matrix. Here, the constraint $C \geq 0$ welcomes positive values on the entries corresponding to the data points from the same subspace while suppressing the entries corresponding to the data points from different subspaces, thus making the coefficient matrix C discriminative. The constraint $\mathbf{1}^\top C = s\mathbf{1}^\top$ limits the sum of each coefficient vector c_i to be s , and thus make the representation more discriminative due to the fact that each entry should be non-negative.

B. Model Optimization

The proposed SRLSR model (9) can not be solved in an analytical form. In this section, we solve it by employing the variable splitting methods [44], [45]. Specifically, we introduce an auxiliary variable Z into the SRLSR model (9), which can then be equivalently reformulated as a linear equality-constrained problem:

$$\begin{aligned} \min_{C, Z} & \|X - XC\|_F^2 + \lambda \|Z\|_F^2 \\ \text{s.t. } & Z \geq 0, \mathbf{1}^\top Z = s\mathbf{1}^\top, Z = C, \end{aligned} \quad (10)$$

whose solution w.r.t. C coincides with the solution of (9). Since the objective function in Eq. (10) is separable w.r.t. the variables C and Z , it can be solved via the alternating direction method of multipliers (ADMM) [36]. The corresponding augmented Lagrangian function is

$$\begin{aligned} \mathcal{L}(C, Z, \Delta, \rho) &= \|X - XC\|_F^2 + \lambda \|Z\|_F^2 + \langle \Delta, Z - C \rangle + \frac{\rho}{2} \|Z - C\|_F^2 \\ &= \|X - XC\|_F^2 + \lambda \|Z\|_F^2 + \frac{\rho}{2} \|Z - C\|_F^2 + \frac{1}{\rho} \Delta^\top (Z - C) \\ &= \|X - XC\|_F^2 + \frac{2\lambda + \rho}{2} \|Z\|_F^2 - \frac{\rho}{2\lambda + \rho} (C - \frac{1}{\rho} \Delta)^\top Z \\ &\quad + \frac{\lambda\rho}{2\lambda + \rho} \|C - \frac{1}{\rho} \Delta\|_F^2, \end{aligned} \quad (11)$$

where Δ is the augmented Lagrangian multiplier and $\rho > 0$ is the penalty parameter. Denote by (C_k, Z_k) and Δ_k the optimization variables and the Lagrange multiplier at iteration k ($k = 0, 1, 2, \dots$), respectively. We initialize the variables C_0 , Z_0 , and Δ_0 to be comfortable zero matrices. By taking derivatives of the Lagrangian function \mathcal{L} w.r.t. C and Z , and setting the derivatives to be zeros, we can alternatively update the variables as follows:

(1) Updating C while fixing Z_k and Δ_k :

The update of C is to solve the following problem:

$$C_{k+1} = \arg \min_C \|X - XC\|_F^2 + \frac{\rho}{2} \|C - (Z_k + \frac{1}{\rho} \Delta_k)\|_F^2. \quad (12)$$

Algorithm 1: Projection of vector u_{k+1} onto a simplex

Input: Data point $u_{k+1} \in \mathbb{R}^N$, scalar s ;
 1. Sort u_{k+1} into w : $w_1 \geq w_2 \geq \dots \geq w_N$;
 2. Find $\alpha = \max\{1 \leq j \leq N : w_j + \frac{1}{j}(s - \sum_{i=1}^j w_i) > 0\}$;
 3. Define $\beta = \frac{1}{\alpha}(s - \sum_{i=1}^{\alpha} w_i)$;
Output: z_{k+1} : $z_{k+1}^i = \max\{u_{k+1}^i + \beta, 0\}$, $i = 1, \dots, N$.

Algorithm 2: Solve the SRLSR model (10) via ADMM

Input: Data matrix X , Tol > 0 , $\rho > 0$, K ;
Initialization: $C_0 = Z_0 = \Delta_0 = \mathbf{0}$, T = False, $k = 0$;
While (T == False) **do**
 1. Update C_{k+1} by Eqn. (13);
 2. Update Z_{k+1} by Eqn. (14);
 3. Update Δ_{k+1} by Eqn. (15);
 4. **if** (Convergence condition is satisfied) or ($k \geq K$)
 T \leftarrow True
end if
end while
Output: Matrices C and Z .

This is a standard least square regression problem and has a closed-form solution given by

$$C_{k+1} = (X^\top X + \frac{\rho}{2} I)^{-1} (X^\top X + \frac{\rho}{2} Z_k + \frac{1}{2} \Delta_k). \quad (13)$$

(2) Updating Z while fixing C_k and Δ_k :

The update of Z is to solve the following problem:

$$\begin{aligned} Z_{k+1} &= \arg \min_Z \|Z - \frac{\rho}{2\lambda + \rho} (C_{k+1} - \rho^{-1} \Delta_k)\|_F^2 \\ \text{s.t. } & Z \geq 0, \mathbf{1}^\top Z = s\mathbf{1}^\top. \end{aligned} \quad (14)$$

This is a quadratic program and the objective function is strictly convex with a close and convex constraint, so there is a unique solution. In fact, the problem (14) can be solved by active set methods [46], [47] and projection based methods [48]–[50], etc. Here, we employ a projection based method [49] whose computational complexity is $\mathcal{O}(N \log N)$ to project a vector of length N onto a simplex. Denote by u_{k+1} an arbitrary column of $\frac{\rho}{2\lambda + \rho} (C_{k+1} - \rho^{-1} \Delta_k)$, the solution of z_{k+1} (the corresponding column in Z_{k+1}) can be solved by projecting u_{k+1} onto a simplex [49]. The solution of problem (14) is summarized in Algorithm 1.

(3) Updating Δ while fixing C_k and Z_k :

$$\Delta_{k+1} = \Delta_k + \rho(Z_{k+1} - C_{k+1}). \quad (15)$$

We repeat the above alternative updates until certain convergence condition is satisfied or the number of iterations reaches a preset threshold K . The convergence condition of the ADMM algorithm is: $\|C_{k+1} - Z_{k+1}\|_F \leq \text{Tol}$, $\|C_{k+1} - C_k\|_F \leq \text{Tol}$, and $\|Z_{k+1} - Z_k\|_F \leq \text{Tol}$ are simultaneously satisfied, where Tol > 0 is a small tolerance value. Since the objective function and constraints are convex, the problem (10) solved by the ADMM algorithm is guaranteed to converge to a global optimal solution. We summarize the updating procedures in Algorithm 2.

C. Discussion

The constraint of “ $\mathbf{1}^\top c = 1$ ” has been already used in the work of Sparse Subspace Clustering (SSC) [15], [16] to deal with affine subspaces instead of linear subspaces. However,

limiting the sum of the coefficient vector \mathbf{c} to be 1 is not flexible enough for real-world clustering problems. What's more, suppressing the sum of the entries in the coefficient vector \mathbf{c} can make it more discriminative, since these entries should be non-negative but sum up to a scalar s . Considering the extreme case that s is nearly zero, each data point must be represented by its most similar data points in the homogeneous subspace. To this end, in our proposed SRLSR model, we extend the affine constraint of "summing up to 1" to a scaled affine constraint of "summing up to a scalar s ". According to our experiments (please refer to Section IV), this extension can indeed improve the performance of SC.

To better illustrate the advantages of SR, in Figure 1 we show an example of three subspaces \mathcal{S}_1 (red), \mathcal{S}_2 (green), and \mathcal{S}_3 (blue) lying in \mathbb{R}^3 . Denote by \mathbf{O} the origin point in \mathbb{R}^3 and set the scalar $s = 0.5$. For simplicity, we assume that there are only two data points in each subspace, and the six points $\{\mathbf{x}_1, \dots, \mathbf{x}_6\}$ satisfy $\mathbf{x}_3 = -\mathbf{x}_4$ and $\mathbf{x}_1 = \mathbf{x}_3 + \mathbf{x}_5$. The coefficients of the data point \mathbf{x}_1 over the others can be solved under different cases. In the "Sparse" case of Figure 1, the coefficients solved by the Lasso model [51] are non-zero over the points \mathbf{x}_4 and \mathbf{x}_5 . In the "Non-negative" case of Figure 1, we compute the coefficients by the Lasso model [51] with a non-negative constraint. Due to the non-negative constraint, the obtained coefficients are non-zero over \mathbf{x}_3 and \mathbf{x}_5 . In the "Affine" case of Figure 1, we compute the coefficients by the Lasso model [51] with an affine constraint. Since the sum of coefficients is 1, the data point \mathbf{x}_1 can only be perfectly represented by itself. All these three cases fail to find the correct subspace since $\mathbf{x}_1 \in \mathcal{S}_1$, while $\mathbf{x}_3, \mathbf{x}_4, \mathbf{x}_5 \notin \mathcal{S}_1$. However, in the "Simplex" case of Figure 1, one can see that the coefficients solved by the proposed SRLSR algorithm are only non-zero over \mathbf{x}_2 , which also belongs to \mathcal{S}_1 as \mathbf{x}_1 , and hence the points $\mathbf{x}_1, \mathbf{x}_2$ can be correctly clustered into the same subspace.

D. Subspace Clustering via Simplex Representation

1) Subspace Clustering Algorithm

Denote by $\mathcal{X} = \{\mathbf{x}_i \in \mathbb{R}^D\}_{i=1}^N$ a set of data points drawn from a union of n subspaces $\{\mathcal{S}_j\}_{j=1}^n$. Most existing spectral clustering based SC algorithms [16], [18], [20], [24], [28], [31] first compute the coefficient matrix \mathbf{C} , and then construct a non-negative affinity matrix \mathbf{A} from \mathbf{C} by exponentiation [14], absolutely symmetrization [15], [16], [20], [23]–[28], [30], [31], or squaring operations [17], [18], [32], etc. On the contrary, in our proposed SRLSR model, the coefficient matrix is guaranteed to be non-negative by the introduced simplex constraint. Hence, we can remove the absolute operation and construct the affinity matrix by a simple symmetrizing operation:

$$\mathbf{A} = \frac{\mathbf{C} + \mathbf{C}^\top}{2}. \quad (16)$$

As a common post-processing step in [15]–[18], [20], [23]–[28], [30]–[32], we apply the spectral clustering technique [42] to the affinity matrix \mathbf{A} , and obtain the final segmentation of data points. Specifically, we employ the widely used Normalized Cut algorithm [43] to segment the affinity matrix.

Algorithm 3: Subspace Clustering by SRLSR

Input: A set of data points $\mathcal{X} = \{\mathbf{x}_1, \dots, \mathbf{x}_N\}$ lying in a union of n subspaces $\{\mathcal{S}_j\}_{j=1}^n$;

1. Obtain the coefficient matrix \mathbf{C} by solving the SRLSR model:
$$\min_{\mathbf{C}} \|\mathbf{X} - \mathbf{X}\mathbf{C}\|_F^2 + \lambda \|\mathbf{C}\|_F^2 \text{ s.t. } \mathbf{C} \geq 0, \mathbf{1}^\top \mathbf{C} = s\mathbf{1}^\top;$$
2. Construct the affinity matrix by

$$\mathbf{A} = \frac{\mathbf{C} + \mathbf{C}^\top}{2};$$

3. Apply spectral clustering [42] to the affinity matrix;

Output: Segmentation of data: $\mathbf{X}_1, \dots, \mathbf{X}_n$.

The proposed SRLSR based subspace clustering algorithm is summarized in Algorithm 3.

2) Complexity Analysis

Assume that there are N data points in the data matrix \mathbf{X} . In Algorithm 2, the costs for updating \mathbf{C} and \mathbf{Z} are $\mathcal{O}(N^3)$ and $\mathcal{O}(N^2 \log N)$, respectively. The costs for updating Δ and ρ can be ignored compared with the updating of \mathbf{C} and \mathbf{Z} . So the overall complexity of Algorithm 2 is $\mathcal{O}(N^3 K)$, where K is the number of iterations. The costs for affinity matrix construction and spectral clustering in Algorithm 3 can be ignored. Hence, the overall cost of the proposed SRLSR method is $\mathcal{O}(N^3 K)$ for data matrix $\mathbf{X} \in \mathbb{R}^{D \times N}$.

IV. EXPERIMENTS

In this section, we evaluate the proposed SRLSR method for the subspace clustering (SC) problem. The evaluations are presented using two protocols. On one hand, we validate the effectiveness of non-negativity and scaled affinity in the simplex constraint. On the other hand, we compare the proposed SRLSR with state-of-the-art SC methods. Both the validation and comparison are performed on three real-world SC problems: motion segmentation for video analysis, human faces clustering, and handwritten digit clustering.

A. Implementation Details

The proposed SRLSR model (9) is solved under the ADMM [36] framework. There are four parameters to be determined in the ADMM algorithm: the regularization parameter λ , the sum s of the entries in the coefficient vector, the penalty parameter ρ and the iteration number K in ADMM algorithm. In all the experiments, we fix $s = 0.5$, $K = 5$ and $\rho = 0.5$. As in most of the competing methods [6], [14]–[18], [20], [23]–[32], the parameter λ will be tuned on each dataset to achieve the best performance of SRLSR on that dataset, which will be introduced in Section IV-D. We also tune the parameter s to see the best performance of SRLSR on that dataset. All experiments are run under the Matlab2014b environment on a machine with Inter(R) Core(TM) i7-4770K CPU of 3.50GHz and 12GB RAM. The code will be released with the publication of this work.

B. Datasets

We evaluate the proposed SRLSR method and the competing methods on the Hopkins 155 dataset [37] for motion segmentation, the Extended Yale B dataset [38] for human face clustering, and the MNIST dataset [39] for handwritten digit clustering.

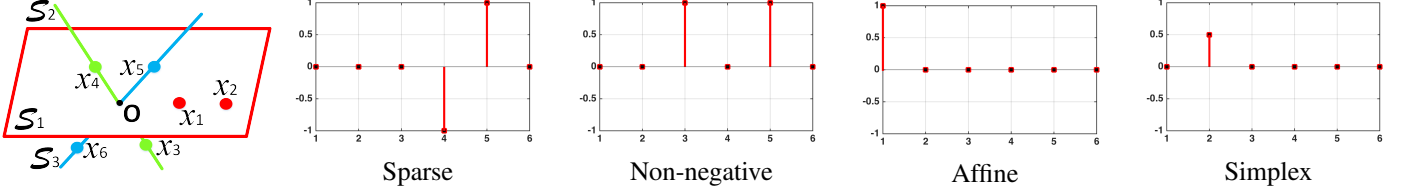


Fig. 1: An example of three subspaces in \mathbb{R}^3 with two data points in each subspace, i.e., $x_1, x_2 \in \mathcal{S}_1$, $x_3, x_4 \in \mathcal{S}_2$, and $x_5, x_6 \in \mathcal{S}_3$, respectively. The solution of the Lasso model [51] for data point x_1 is shown in the “Sparse” case. If we add a non-negative constraint into the Lasso model [51], the result is shown in the “Non-negative” case. The solution of the Lasso model [51] with the affine constraint for data point x_1 is shown in the “Affine” case. As shown in the “Simplex” case, the proposed SRLSR algorithm can find the correct data point x_2 , which is in the same subspace of x_1 .

The **Hopkins 155** dataset [37] contains 155 video sequences, 120 of which contain two moving objects and 35 of which contain three moving objects, corresponding to 2 or 3 low-dimensional subspaces of the ambient space. On average, each sequence of two motions has $N = 266$ data points of 30 frames, while each sequence of three motions has $N = 393$ data points with 29 frames. Similar to the experimental settings in previous methods such as SSC [16], on this dataset we employ the principal component analysis (PCA) [52] to project the original trajectories of different objects into a 12-dimensional subspace, in which we evaluate the comparison methods.

The **Extended Yale B** dataset [38] contains face images of 38 human subjects, each subject has 64 near frontal images (gray scale) taken under different illumination conditions. The original images are of size 192×168 and we resize the images to 48×42 pixels in our experiments. The resized images are further projected onto a $6n$ -dimensional subspace by using PCA, where n is the number of subjects (or subspaces) we choose in our experiments. As the experimental settings in SSC [16], we divide the 38 subjects into 4 groups corresponding to subjects 1 to 10, subjects 11 to 20, subjects 21 to 30, and subjects 31 to 38, respectively. For each of the first three groups we consider choices of $n \in \{2, 3, 5, 8, 10\}$ subjects, and for the last group we consider choices of $n \in \{2, 3, 5, 8\}$. Finally, we apply SC algorithms for each set of n subjects.

The **MNIST** dataset [39] contains 60,000 gray scale images of 10 digits (i.e., $\{0, \dots, 9\}$) in the training set and 10,000 images in the testing set. The images are of size 28×28 . In our experiments, we randomly select $N_i \in \{50, 100, 200, 400, 600\}$ images for each of the 10 digits. For each image, a set of feature vectors is computed using the scattering convolution network (SCN) [53]. The final feature vector for that image is a concatenation of coefficients in each layer of the network, and is translation invariant and deformation stable. Each feature vector is of 3,472-dimension. The feature vectors for all images are then projected onto a 500-dimensional subspace by using PCA.

C. Ablation Study: Effectiveness of Simplex Representation

We perform comprehensive ablation studies on the three commonly used datasets to validate the effectiveness of the proposed SRLSR model. The SRLSR includes two constraints, i.e., $c \geq 0$ and $\mathbf{1}^\top c = s$. To analyze the effectiveness of each

constraint, we compare the clustering errors of the proposed SRLSR model with several baseline methods.

The first baseline is the trivial Least Square Regression (LSR) model as follows:

$$\text{LSR: } \min_C \|X - XC\|_F^2 + \lambda \|C\|_F^2. \quad (17)$$

By removing each individual constraint in the simplex constraint from the proposed SRLSR model (9), we have the second baseline method, called the Non-negative Least Square Regression (NLSR) model:

$$\text{NLSR: } \min_C \|X - XC\|_F^2 + \lambda \|C\|_F^2 \quad \text{s.t. } C \geq 0. \quad (18)$$

The NLSR model can be formulated by either removing the scaled affinity constraint $\mathbf{1}^\top c = s$ from SRLSR or adding a non-negative constraint to the LSR model (17). For structural integration of this paper, we put the solution of the NLSR model (18) in Appendix A. We can also remove the non-negative constraint $C \geq 0$ in the scaled simplex set $\{C \in \mathbb{R}^{N \times N} | C \geq 0, \mathbf{1}^\top C = s\mathbf{1}^\top\}$, and obtain a Scaled-affine Least Square Regression (SLSR) model:

$$\text{SLSR: } \min_C \|X - XC\|_F^2 + \lambda \|C\|_F^2 \quad \text{s.t. } \mathbf{1}^\top C = s\mathbf{1}^\top. \quad (19)$$

The solution of the SLSR model (19) is given in Appendix B. To validate the effectiveness of scaled-affinity over the trivial affine constraint, we introduce the Affine constrained Least Square Regression (ALSR) model as another baseline method for SC. The ALSR can be formulated as follows:

$$\text{ALSR: } \min_C \|X - XC\|_F^2 + \lambda \|C\|_F^2 \quad \text{s.t. } \mathbf{1}^\top C = \mathbf{1}^\top. \quad (20)$$

The affinity in ALSR can also be explained from the perspective of probability simplex constraint: the aim is to obtain a set of non-negative coefficients summed to 1, like a probability distribution function. The solution of the ALSR model (20) is similar to that of the SLSR model (19) when $s = 1$.

The proposed SRLSR method as well as the four baseline methods can be expressed in a standard form:

“ $\min_C \text{Data Term} + \text{Regularization Term}$ s.t. Constraints ”. In the methods of NLSR, SLSR, ALSR, and SRLSR, the data and regularization terms are the same as those of the basic LSR model, i.e., $\|X - XC\|_F^2$ and $\lambda \|C\|_F^2$, respectively. The difference among these comparison methods lies

in the *Constraints*. We summarize the proposed SRLSR as well as the four baseline methods LSR, NLSR, SLR, and ALSR in Table I.

In Tables II-IV, we list the average clustering errors (%) of the proposed SRLSR and the four baseline methods on the Hopkins 155 dataset [37], the Extended Yale B dataset [38], and the MNIST dataset [39]. Note that here we tune the parameter s to achieve the best performance of SRLSR on different datasets.

1) Effectiveness of the Non-negative Constraint

The effectiveness of the non-negative constraint $C \geq 0$ in the proposed SRLSR model can be validated from two complementary aspects. First, we can validate the effectiveness of the non-negative constraint by evaluating the performance improvement of the baseline NLSR (18) over LSR [23]. Since the only difference between the baseline methods LSR (17) and NLSR (18) is the additional non-negative constraint in NLSR (18), the performance gain of NLSR over LSR can directly reflect the effectiveness of the non-negative constraint. Second, the effectiveness of the non-negative constraint can also be validated by comparing the performance of the proposed SRLSR (9) and the baseline method SLR (19). Since the only difference between the two methods is that SLR (19) lacks a non-negative constraint, the performance gain of SRLSR over SLR can reflect the usefulness of the non-negative property.

From the results listed in Table II, one can see that, on the Hopkins 155 dataset the baseline methods LSR and NLSR achieve average clustering errors of 3.67% and 1.75%, respectively. This demonstrates that by adding the non-negative constraint to LSR, the resulting baseline NLSR reduces significantly the clustering error. Besides, the average clustering errors of SRLSR ($s = 0.9$) and SLR are 1.04% and 3.16%, respectively. This demonstrates that if we remove the non-negative constraint from the SRLSR model, the resulting SLR model will drop a lot the clustering performance. Similar trends can be found from Tables III and IV on the Extended Yale B dataset [38] and the MNIST dataset [39], respectively. All these comparisons demonstrate that the non-negative constraint is an essential factor for the success of the proposed SRLSR method.

2) Effectiveness of the Scaled-Affine Constraint

The effectiveness of the scaled-affine constraint can be validated from three aspects. First, we can validate the scaled affine constraint by comparing the baseline methods LSR (17) and SLR (19), which are summarized in Table I. Since the only difference between LSR (17) and SLR (19) is that SLR contains an additional scaled affine constraint over LSR, the performance gain of SLR over LSR can directly validate the effectiveness of scaled affine constraint. Second, the effectiveness can be validated by comparing the proposed SRLSR (9) and the baseline NLSR (18). This is because NLSR can be formulated by removing the scaled affine constraint from SRLSR. Third, we can also validate the advantages of scaled affine constraint over affine constraint by comparing the baseline methods SLR (19) and ALSR (20).

From the results listed in Tables II, we can observe that, on the Hopkins 155 dataset [37], the proposed SRLSR ($s = 0.9$)

can achieve lower clustering error (1.04%) than the baseline method NLSR (1.75%). Similar conclusions can be found in Tables III and IV for the experiments on the Extended Yale B dataset [38] and the MNIST dataset [39], respectively. All these comparisons demonstrate that the scaled affine constraint is another essential factor for the success of SRLSR.

3) Effectiveness of the Simplex Constraint

We find that the proposed simplex constraint, i.e., the integration of the non-negative and scaled affine constraints, can further boost the performance of SC. This can be validated by comparing the performance of the proposed SRLSR (9) and the baseline method LSR (17). From the results listed in Tables II-IV, one can see that on all the three commonly used datasets, the proposed SRLSR can achieve much lower clustering errors than the baseline method LSR. For example, on the MNIST dataset, the clustering errors of SRLSR ($s = 0.15$) are 10.29%, 5.40%, 4.36%, 3.09%, 2.52% when we randomly select 50, 100, 200, 400, 600 images for each of the 10 digits, respectively. Meanwhile, the corresponding clustering errors of the baseline method LSR are 24.98%, 20.24%, 20.56%, 22.24%, 20.12%, respectively. The SRLSR performs much better than LSR in all cases. Similar trends can also be found on the Hopkins 155 dataset (Table II) and the Extended Yale B dataset (Table III).

D. Comparison with State-of-the-art Methods

1) Comparison Methods

We compare the proposed SRLSR with several state-of-the-art SC methods, including SSC [15], [16], LRR [17], [18], LRSC [20], LSR [23], SMR [24], S3C [28], [29], RSIM [6], and SSCOMP [31]. For SRLSR, we provide the results when fixing $s = 0.5$, and those reported in ablation study, i.e., $s = 0.9$ on Hopkins 155, $s = 0.25$ on Extended YaleB, and $s = 0.15$ on MNIST. For the SMR method, we use the J_1 affinity matrix (i.e., (7) in Section II) as described in [24] for fair comparison. For the other methods, we tune their corresponding parameters on each of the three datasets, i.e., the Hopkins 155 dataset [37] for motion segmentation, the Extended Yale B dataset [38] for face clustering, and the MNIST dataset [39] for handwritten digit clustering, to achieve their best clustering results.

2) Comparison on Affinity Matrix

The affinity matrix plays a key role to the success of SC algorithms. In this section, we visualize the affinity matrix of the proposed SRLSR and the comparison methods on SC problem. We run the proposed SRLSR algorithm and the competing methods [6], [16], [18], [20], [23], [28], [29], [31] on the MNIST dataset [39]. The training set contains 6,000 images for each digit in $\{0, 1, \dots, 9\}$. We randomly select 50 images for each digit, and use the total 500 images to construct the affinity matrices by these competing SC methods. The affinity matrices of these methods are visualized in Figure 2, from which one can see that the affinity matrices of SRLSR show better connection within each subspace, and generate less noise than most of the other methods. Though LSR [23] and RSIM [6] show less noise than our proposed SRLSR, their affinity matrices suffer from strong diagonal entries,

TABLE I: Summary of the proposed SRLSR and four baseline methods LSR, NLSR, SLSR and ALSR.

Model	Data Term	Regularization Term	Constraints		Solution
			Non-negativity	Scaled-affinity	
LSR (17)	$\ \mathbf{X} - \mathbf{X}\mathbf{C}\ _F^2$	$\lambda\ \mathbf{C}\ _F^2$	-	-	$\hat{\mathbf{C}} = (\mathbf{X}^\top \mathbf{X} + \lambda \mathbf{I})^{-1} \mathbf{X}^\top \mathbf{X}$
NLSR (18)	$\ \mathbf{X} - \mathbf{X}\mathbf{C}\ _F^2$	$\lambda\ \mathbf{C}\ _F^2$	$\mathbf{C} \geq 0$	-	See Appendix A
SLSR (19)	$\ \mathbf{X} - \mathbf{X}\mathbf{C}\ _F^2$	$\lambda\ \mathbf{C}\ _F^2$	-	$\mathbf{1}^\top \mathbf{C} = s\mathbf{1}^\top$	See Appendix B
ALSR (20)	$\ \mathbf{X} - \mathbf{X}\mathbf{C}\ _F^2$	$\lambda\ \mathbf{C}\ _F^2$	-	$\mathbf{1}^\top \mathbf{C} = \mathbf{1}^\top$	Solving SLSR (19) with $s = 1$
SRLSR (9)	$\ \mathbf{X} - \mathbf{X}\mathbf{C}\ _F^2$	$\lambda\ \mathbf{C}\ _F^2$	$\mathbf{C} \geq 0$	$\mathbf{1}^\top \mathbf{C} = s\mathbf{1}^\top$	See Section III-B

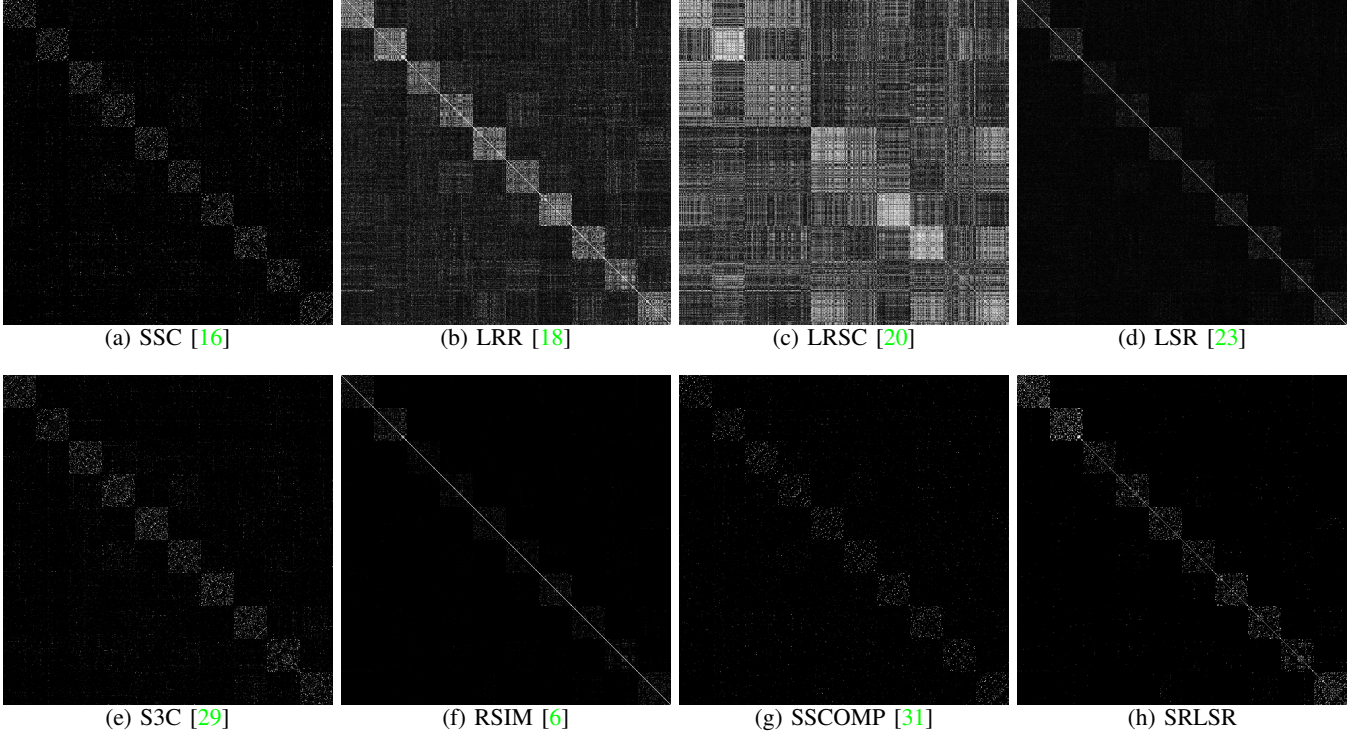


Fig. 2: Affinity matrices computed by SSC [16], LRR [18], LRSC [20], LSR [23], S3C [28], [29], RSIM [6], SSCOMP [31], and the proposed SRLSR on the handwritten digit images from the MNIST dataset [39]. 50 images for each digit of $\{0, 1, \dots, 9\}$ are used to compute the affinity matrix by different methods. All images are normalized to $[0, 1]$ by dividing the maximal entries in corresponding affinity matrices.

TABLE II: Average clustering errors (%) of LSR, NLSR, SLSR, ALSR, and SRLSR ($s = 0.9$) on the Hopkins 155 dataset [37] with the 12-dimensional data points obtained by applying PCA.

	LSR	NLSR	SLSR	ALSR	SRLSR
Error (%)	3.67	1.75	3.16	3.28	1.04

indicating that by these two methods the data points are mainly reconstructed by themselves. As will be demonstrated in the following sections, with the simplex constraint, the proposed SRLSR algorithm can exploit better the inherent correlations among the data points and achieve better clustering performance than the other competing SC algorithms.

3) Results on Motion Segmentation

The Hopkins 155 dataset [37] has been widely used as a benchmark to evaluate the SC methods for the motion segmen-

TABLE III: Average clustering errors (%) of LSR, NLSR, SLSR, ALSR, and SRLSR ($s = 0.25$) on the Extended Yale B dataset [38] with the $6n$ -dimensional (n is the number of subjects) data points obtained by applying PCA.

n	LSR	NLSR	SLSR	ALSR	SRLSR
2	4.98	3.46	4.35	5.26	0.96
3	6.87	4.95	6.56	8.88	1.32
5	14.14	10.03	13.77	17.70	2.22
8	24.39	17.74	22.14	28.54	3.00
10	28.59	20.29	26.31	34.90	3.18

tation problem. Figure 3 presents some example segmentations from the Hopkins 155 dataset [37], where different colors indicate different moving objects and persons, etc.

We first study how the parameter s influences the average clustering errors of the proposed SRLSR algorithm. The

TABLE IV: Average clustering errors (%) of LSR, NLSR, SLSR, ALSR, and SRLSR ($s = 0.15$) on the MNIST dataset [39]. The features of data points are extracted from a scattering network and projected onto a 500-dimensional subspace obtained by applying PCA. The experiments are independently repeated for 20 times.

# of Images	LSR	NLSR	SLSR	ALSR	SRLSR
500	24.98	15.29	22.00	23.12	10.29
1,000	20.24	12.66	18.59	19.89	5.40
2,000	20.56	10.13	16.87	17.58	4.36
4,000	22.24	9.07	15.48	16.34	3.09
6,000	20.12	8.34	14.23	15.79	2.52



Fig. 3: Some exemplar results of motion segmentation from the Hopkins 155 dataset [37].

clustering errors with respect to the value of s are plotted in Figure 4, from which one can see that the proposed SRLSR achieves average clustering error of 1.53% when setting $s = 0.5$, better than all previous methods. Note that SRLSR can achieve the lowest average clustering error of 1.04% when the scalar s is set as $s = 0.9$. The parameter λ is set as $\lambda = 0.001$. We then compare the proposed SRLSR with the other competing SC algorithms [6], [16], [18], [20], [23], [24], [28], [29], [31]. The results of average clustering errors are listed in Table V, from which we can see that the proposed SRLSR achieves the lowest clustering error. Besides, the speed of the proposed SRLSR approach is only slightly slower than LRSC, LSR, and SSCOMP, but much faster than the other competing methods.

4) Results on Human Face Clustering

In this section, we compare the proposed SRLSR algorithm with the competing methods on the commonly used Extended Yale B dataset [38] for human face clustering. Figure 5 shows some face images of this dataset captured under different lighting conditions. For dimensional reduction purpose, the original 48×42 face images are projected onto a $6n$ -dimensional (n is the number of subjects) subspace by applying PCA.

We first study how the scalar s influences the clustering errors (%) of the proposed SRLSR algorithm. The average

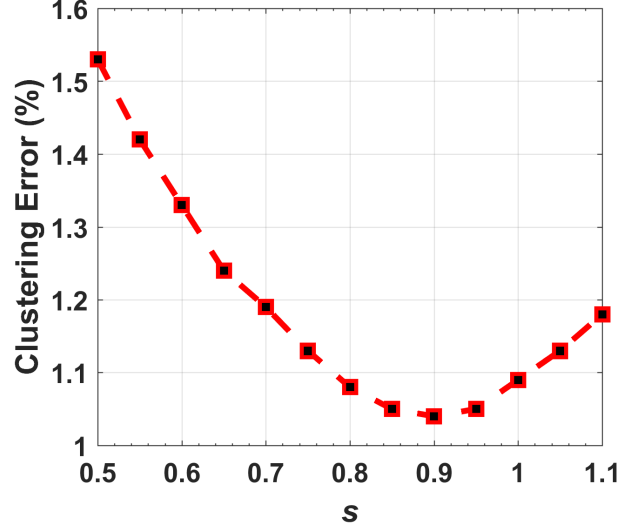


Fig. 4: The influence of scalar s on the average clustering errors (%) of the proposed SRLSR algorithm on the Hopkins 155 dataset [37].



Fig. 5: Some face images from the Extended Yale B dataset [38].

clustering errors with respect to the value of s are plotted in Figure 6. One can see that SRLSR achieves average clustering error of 3.26% when setting $s = 0.5$, and achieves its lowest average clustering errors of 2.16% when $s = 0.25$. The parameter λ is set as $\lambda = 0.005$. The comparison results of different algorithms are listed in Table IV. We can observe that, on different number ($\{2, 3, 5, 8, 10\}$) of clustering subjects, the average clustering errors of SRLSR are always much lower than the other competing methods. For example, when clustering 10 subjects, the average error of SRLSR (when fixing $s = 0.5$) is 5.10%, while the results of the other methods are 10.94% for SSC, 28.54% for LRR, 30.05% for LRSC, 28.59% for LSR, 28.18% for SMR, 5.16% for S3C, 6.56% for RSIM, and 14.80% for SSCOMP, respectively. The performance gain of SRLSR (5.10%) over LSR (28.59%) demonstrates the power of simplex representation on human face clustering. On running time, one can see that the proposed SRLSR algorithm is efficient and comparable to SSCOMP, which is the most efficient algorithm among all competing methods.

TABLE V: Average clustering errors (%) and running time (second) of different algorithms on the Hopkins 155 dataset [37] with the 12-dimensional data points obtained by applying PCA.

Algorithms	SSC [16]	LRR [18]	LRSC [20]	LSR [23]	SMR [24]	S3C [29]	RSIM [6]	SSCOMP [31]	SRLSR	SRLSR ($s = 0.9$)
Error (%)	2.18	3.28	5.41	2.33	2.27	2.61	1.76	25.35	1.53	1.04
Time (s)	0.49	0.28	0.04	0.05	0.35	2.86	0.18	0.06	0.07	0.07

TABLE VI: Average clustering errors (%) and running time (second) of different algorithms on the Extended Yale B dataset [38] with the $6n$ -dimensional (n is the number of subjects) data points obtained by applying PCA.

# of Subjects	2 Subjects		3 Subjects		5 Subjects		8 Subjects		10 Subjects	
	Error (%)	Time (s)	Error (%)	Time (s)	Error (%)	Time (s)	Error (%)	Time (s)	Error (%)	Time (s)
SSC [16]	1.86	0.17	3.10	0.31	4.31	0.74	5.85	2.72	10.94	4.27
LRR [18]	4.99	0.15	6.86	0.29	14.04	0.65	24.18	1.30	28.54	1.81
LRSC [20]	4.42	0.03	6.14	0.06	13.06	0.13	24.12	0.28	30.05	0.45
LSR [23]	4.98	0.03	6.87	0.05	14.14	0.12	24.39	0.25	28.59	0.36
SMR [24]	4.68	0.21	6.56	0.30	13.78	0.76	24.25	2.00	28.18	2.59
S3C [29]	1.27	1.31	2.71	2.58	3.41	3.52	4.13	7.14	5.16	13.98
RSIM [6]	2.17	0.09	2.96	0.17	4.13	0.47	5.82	1.77	6.56	3.19
SSCOMP [31]	2.76	0.03	5.35	0.04	7.89	0.08	11.40	0.19	14.80	0.27
SRLSR	1.26	0.03	1.58	0.04	2.70	0.08	5.66	0.18	5.10	0.28
SRLSR ($s = 0.25$)	0.96	0.03	1.32	0.04	2.22	0.08	3.00	0.18	3.18	0.28

TABLE VII: Average clustering errors (%) and running time (second) of different algorithms on the MNIST dataset [39]. The features are extracted from a scattering network and projected onto a 500-dimensional subspace by applying PCA. The experiments are repeated for 20 times and the average results are reported.

# of Images	500		1,000		2,000		4,000		6,000	
	Error (%)	Time (s)	Error (%)	Time (s)	Error (%)	Time (s)	Error (%)	Time (s)	Error (%)	Time (s)
SSC [16]	16.99	27.36	15.95	49.25	14.42	94.84	14.00	239.95	14.40	423.47
LRR [18]	17.97	15.64	16.88	28.14	16.63	54.19	15.42	137.11	15.45	241.98
LRSC [20]	24.16	0.34	21.58	0.96	21.91	4.74	20.94	27.40	20.09	78.21
LSR [23]	24.98	0.29	20.24	0.91	20.56	4.74	22.24	28.86	20.12	83.14
SMR [24]	18.45	19.56	13.97	35.18	9.46	67.75	9.14	171.39	7.36	302.48
S3C [29]	15.92	135.20	12.23	263.33	10.54	521.93	9.46	1308.50	9.34	2544.41
RSIM [6]	18.13	10.06	15.70	18.09	11.48	34.84	10.53	88.14	10.21	155.56
SSCOMP [31]	16.36	0.32	13.33	0.88	9.40	4.50	8.78	26.94	8.75	76.84
SRLSR	11.81	0.35	6.90	1.02	5.65	5.23	5.31	31.42	4.53	89.62
SRLSR ($s = 0.15$)	10.29	0.37	5.40	1.03	4.36	5.25	3.09	31.43	2.52	89.65

5) Results on Handwritten Digit Clustering

For the digit clustering problem, we follow the experimental settings in SSSCOMP [31] and evaluate the competing methods on the MNIST dataset [39]. Figure 7 shows some example of the handwritten digit images. The testing data consist of a randomly chosen number of $N_i \in \{50, 100, 200, 400, 600\}$ images for each of the 10 digits, with features extracted from the scattering convolution network [53]. The extracted features of the digit images are originally 3,472-dimensional and are projected onto a 500-dimensional subspace by applying PCA.

We first evaluate the influence of scalar s on the average clustering errors (%) of SRLSR. The curve of clustering errors w.r.t. s is plotted in Figure 8, in which we compute the average clustering errors of 20 trials sampled from 6,000 randomly selected images ($N_i = 600$). One can see that the proposed SRLSR algorithm achieves an average clustering error of 4.53%, and achieves its lowest average clustering error (2.52%) when $s = 0.15$. The parameter λ is set as

$\lambda = 0.01$. We list the average clustering errors (%) of the competing methods in Table VII, in which the results of other methods are copied from [31]. One can see that the proposed SRLSR algorithm performs better than all the other competing methods. For example, SRLSR achieves clustering errors of 11.81%, 6.90%, 5.65%, 5.31%, and 4.53% when the number of digit images are 500, 1000, 2000, 4000, and 6000, respectively. These results are much better than the other competing algorithms including the recently proposed SSSCOMP, whose clustering errors are 16.36%, 13.33%, 9.40%, 8.78%, and 8.75%, respectively.

V. CONCLUSION

In this paper, we proposed a simplex representation based least square regression (SRLSR) model for spectral clustering based subspace clustering. Specifically, we introduced the non-negative and scaled affine constraints into the least square regression (LSR) model. The proposed SRLSR model can

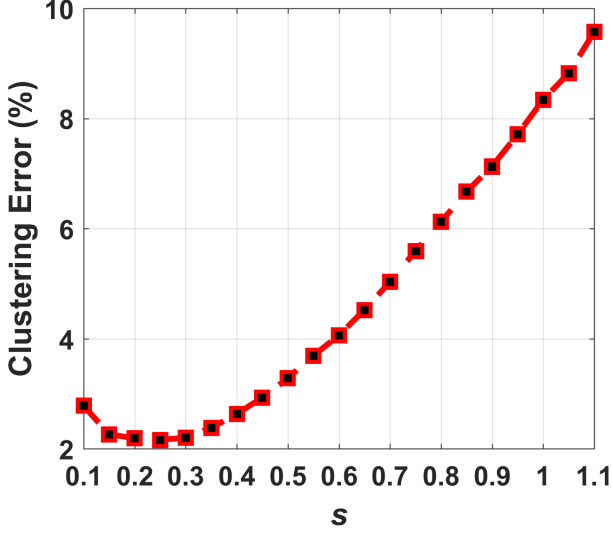


Fig. 6: The influence of scalar s on the average clustering errors (%) of the proposed SRLSR algorithm on the Extended Yale B dataset [38].



Fig. 7: Some digit images from the MNIST dataset [39].

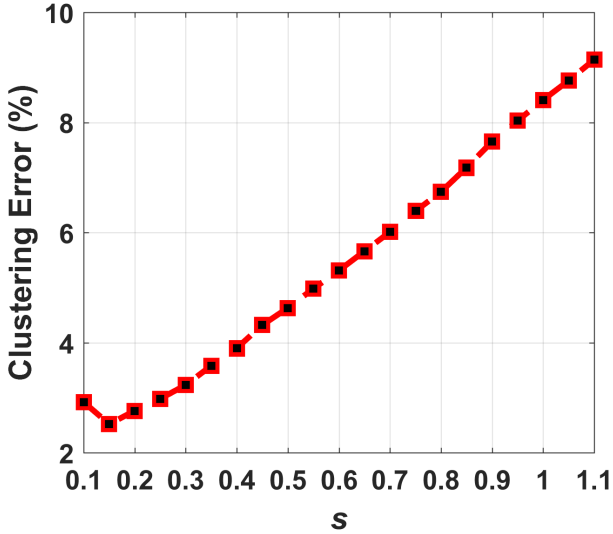


Fig. 8: The influence of scalar s on the average clustering errors (%) of the proposed SRLSR algorithm on the MNIST dataset [39] with 600 images for each digit.

reveal the inherent correlations among the data points while being very discriminative. Based on the SRLSR model, a novel spectral clustering based algorithm was developed for subspace clustering. Extensive experiments on three benchmark clustering datasets demonstrated that the proposed SRLSR algorithm is very efficient and achieves better clustering performance than state-of-the-art subspace clustering algorithms. The significant improvements of SRLSR over the baseline LSR model demonstrate the effectiveness of the introduced

simplex representation.

APPENDIX A SOLUTION OF THE NLSR MODEL (18)

The NLSR model (18) does not have an analytical solution. We employ the variable splitting method [44], [45] to solve the NLSR model (18). By introducing an auxiliary variable Z , we can reformulate the NLSR model (18) into a linear equality-constraint problem with two variables C and Z :

$$\min_{C, Z} \|X - XC\|_F^2 + \lambda \|C\|_F^2 \quad \text{s.t.} \quad Z = C, Z \geq 0. \quad (21)$$

Since the objective function is separable w.r.t. the variables C and Z , the problem (21) can be solved under the alternating direction method of multipliers (ADMM) [36] framework. The Lagrangian function of the problem (21) is

$$\begin{aligned} \mathcal{L}(C, Z, \Delta, \lambda, \rho) = & \|X - XC\|_F^2 + \lambda \|C\|_F^2 \\ & + \langle \Delta, Z - C \rangle + \frac{\rho}{2} \|Z - C\|_F^2, \end{aligned} \quad (22)$$

where Δ is the augmented Lagrangian multiplier and $\rho > 0$ is the penalty parameter. We initialize the vector variables C_0 , Z_0 , and Δ_0 to be zero vector and set $\rho > 0$ with a suitable value. Denote by (C_k, Z_k) and δ_k the optimization variables and the Lagrange multiplier at iteration k ($k = 0, 1, 2, \dots, K$), respectively. The variables can be updated by taking derivatives of the Lagrangian function (22) w.r.t. the variables C and Z and setting the derivative function to be zero.

(1) **Updating C while fixing Z and Δ :**

$$\min_C \|X - XC\|_F^2 + \lambda \|C\|_F^2 + \frac{\rho}{2} \|C - (Z_k + \rho^{-1} \Delta_k)\|_F^2. \quad (23)$$

This is a standard least squares regression problem with closed form solution:

$$C_{k+1} = (X^\top X + \frac{2\lambda + \rho}{2} I)^{-1} (X^\top X + \frac{\rho}{2} Z_k + \frac{1}{2} \Delta_k) \quad (24)$$

(2) **Updating Z while fixing C and Δ :**

$$\min_Z \|Z - (C_{k+1} - \rho^{-1} \Delta_k)\|_F^2 \quad \text{s.t.} \quad Z \geq 0. \quad (25)$$

The solution of Z is

$$Z_{k+1} = \max(0, C_{k+1} - \rho^{-1} \Delta_k), \quad (26)$$

where the “ $\max(\cdot)$ ” operator outputs element-wisely the maximal value of the inputs.

(3) **Updating the Lagrangian multiplier Δ :**

$$\Delta_{k+1} = \Delta_k + \rho(Z_{k+1} - C_{k+1}). \quad (27)$$

The above alternative updating steps are repeated until the convergence condition is satisfied or the number of iterations exceeds a preset threshold K . The convergence condition of the ADMM algorithm is: $\|Z_{k+1} - C_{k+1}\|_F \leq \text{Tol}$, $\|C_{k+1} - C_k\|_F \leq \text{Tol}$, and $\|Z_{k+1} - Z_k\|_F \leq \text{Tol}$ are simultaneously satisfied, where $\text{Tol} > 0$ is a small tolerance value. Since the least square objective function and the linear equality and non-negative constraints are all strictly convex, the problem (21) solved by the ADMM algorithm is guaranteed to converge to a global optimal solution.

Algorithm 4: Projection of the vector \mathbf{v}_{k+1} onto a scaled affine space

Input: Data point $\mathbf{v}_{k+1} \in \mathbb{R}^N$, scalar s .
 1. Sort \mathbf{v}_{k+1} into \mathbf{w} : $w_1 \geq w_2 \geq \dots \geq w_N$;
 2. Find $\alpha = \max\{1 \leq j \leq N : w_j + \frac{1}{j}(s - \sum_{i=1}^j w_i) > 0\}$
 3. Define $\beta = \frac{1}{\alpha}(s - \sum_{i=1}^{\alpha} w_i)$;
Output: \mathbf{z}_{k+1} : $\mathbf{z}_{k+1}^i = \mathbf{v}_{k+1}^i + \beta$, $i = 1, \dots, N$.

APPENDIX B

SOLUTION OF THE SLSR MODEL (19)

In this section we solve the SLSR model (19) by employing the variable splitting methods [44], [45]. Specifically, we introduce an auxiliary variable \mathbf{Z} into the SLSR model (19), which can then be equivalently reformulated as a linear equality-constrained problem:

$$\begin{aligned} \min_{\mathbf{C}, \mathbf{Z}} & \|\mathbf{X} - \mathbf{X}\mathbf{C}\|_F^2 + \lambda \|\mathbf{Z}\|_F^2 \\ \text{s.t.} & \mathbf{1}^\top \mathbf{Z} = s\mathbf{1}^\top, \mathbf{Z} = \mathbf{C}, \end{aligned} \quad (28)$$

whose solution for \mathbf{C} coincides with the solution of (19). Since its objective function is separable w.r.t. the variables \mathbf{C} and \mathbf{Z} , the problem (28) can also be solved via the ADMM method [36]. The corresponding augmented Lagrangian function is the same as Eqn. (11). Denote by $(\mathbf{C}_k, \mathbf{Z}_k)$ and Δ_k the optimization variables and Lagrange multiplier at iteration k ($k = 0, 1, 2, \dots$), respectively. We initialize the variables \mathbf{C}_0 , \mathbf{Z}_0 , and Δ_0 to be comfortable zero matrices. By taking derivatives of the Lagrangian function \mathcal{L} (11) w.r.t. \mathbf{C} and \mathbf{Z} , and setting the derivatives to be zeros, we can alternatively update the variables as follows:

(1) **Updating \mathbf{C} while fixing \mathbf{Z}_k and Δ_k :**

The update on \mathbf{C} is to solve the following problem:

$$\mathbf{C}_{k+1} = \arg \min_{\mathbf{C}} \|\mathbf{X} - \mathbf{X}\mathbf{C}\|_F^2 + \frac{\rho}{2} \|\mathbf{C} - (\mathbf{Z}_k + \frac{1}{\rho} \Delta_k)\|_F^2. \quad (29)$$

This is a standard least square regression problem and has a closed-form solution given by

$$\mathbf{C}_{k+1} = (\mathbf{X}^\top \mathbf{X} + \frac{\rho}{2} \mathbf{I})^{-1} (\mathbf{X}^\top \mathbf{X} + \frac{\rho}{2} \mathbf{Z}_k + \frac{1}{2} \Delta_k). \quad (30)$$

(2) **Updating \mathbf{Z} while fixing \mathbf{C}_k and Δ_k :**

The update on \mathbf{Z} is to solve the following problem:

$$\begin{aligned} \mathbf{Z}_{k+1} &= \arg \min_{\mathbf{Z}} \|\mathbf{Z} - \frac{\rho}{2\lambda + \rho} (\mathbf{C}_{k+1} - \rho^{-1} \Delta_k)\|_F^2 \\ \text{s.t.} & \mathbf{1}^\top \mathbf{Z} = s\mathbf{1}^\top. \end{aligned} \quad (31)$$

This is a quadratic program and the objective function is strictly convex with a close and convex constraint, so there is a unique solution. Here, we employ the projection based method [49] whose computational complexity is $\mathcal{O}(N \log N)$ to process a vector of length N . Denote by \mathbf{v}_{k+1} an arbitrary column of $\frac{\rho}{2\lambda + \rho} (\mathbf{C}_{k+1} - \rho^{-1} \Delta_k)$, the solution of \mathbf{z}_{k+1} (the corresponding column in \mathbf{Z}_{k+1}) can be solved by projecting \mathbf{v}_{k+1} onto a scaled affine space [49]. The solution of the problem (31) is summarized in Algorithm 4.

(3) **Updating Δ while fixing \mathbf{C}_k and \mathbf{Z}_k :**

$$\Delta_{k+1} = \Delta_k + \rho(\mathbf{Z}_{k+1} - \mathbf{C}_{k+1}). \quad (32)$$

We repeat the above alternative updates until certain convergence condition is satisfied or the number of iterations reaches a preset threshold K . The convergence condition of the ADMM algorithm is: $\|\mathbf{C}_{k+1} - \mathbf{Z}_{k+1}\|_F \leq \text{Tol}$, $\|\mathbf{C}_{k+1} - \mathbf{C}_k\|_F \leq \text{Tol}$, and $\|\mathbf{Z}_{k+1} - \mathbf{Z}_k\|_F \leq \text{Tol}$ are simultaneously satisfied, where $\text{Tol} > 0$ is a small tolerance value. Since the objective function and constraints are convex, the problem (28) solved by the ADMM algorithm is guaranteed to converge to a global optimal solution.

REFERENCES

- [1] R. Vidal. A tutorial on subspace clustering. *IEEE Signal Processing Magazine*, 2011. 1
- [2] J. Ho, M.-H. Yang, J. Lim, K.-C. Lee, and D. Kriegman. Clustering appearances of objects under varying illumination conditions. In *CVPR*, pages 11–18, 2003. 1, 2
- [3] Manolis C. Tsakiris and Rene Vidal. Algebraic clustering of affine subspaces. *IEEE Trans. Pattern Anal. Mach. Intell.*, 40(2):482–489, 2018. 1, 2
- [4] J. Costeira and T. Kanade. A multibody factorization method for independent moving objects. *IJCV*, 29(3), 1998. 1, 2
- [5] R. Vidal, Y. Ma, and S. Sastry. Generalized principal component analysis. *IEEE Trans. Pattern Anal. Mach. Intelligence*, 27(12):1–15, 2005. 1, 2
- [6] P. Ji, M. Salzmann, and H. Li. Shape interaction matrix revisited and robustified: Efficient subspace clustering with corrupted and incomplete data. In *ICCV*, pages 4687–4695, 2015. 1, 2, 5, 7, 8, 9, 10
- [7] M. Tipping and C. Bishop. Mixtures of probabilistic principal component analyzers. *Neural Computation*, 11(2):443–482, 1999. 1, 2
- [8] A. Gruber and Y. Weiss. Multibody factorization with uncertainty and missing data using the em algorithm. In *CVPR*, 2004. 1, 2
- [9] M. Fischler and R. Bolles. Random sample consensus: a paradigm for model fitting with applications to image analysis and automated cartography. *Communications of the ACM*, 24(6):381–395, 1981. 1, 2
- [10] S. Rao, R. Tron, R. Vidal, and Y. Ma. Motion segmentation via robust subspace separation in the presence of outlying, incomplete, or corrupted trajectories. *IEEE Trans. Pattern Anal. Mach. Intelligence*, pages 1832–1845, 2009. 1, 2
- [11] J. Yan and M. Pollefeys. A general framework for motion segmentation: Independent, articulated, rigid, non-rigid, degenerate and non-degenerate. *ECCV*, 2006. 1, 2
- [12] T. Zhang, A. Szlam, Y. Wang, and G. Lerman. Hybrid linear modeling via local best-fit flats. *CVPR*, 2010. 1, 2
- [13] A. Goh and R. Vidal. Segmenting motions of different types by unsupervised manifold clustering. *CVPR*, 2007. 1, 2
- [14] G. Chen and G. Lerman. Spectral curvature clustering. *IJCV*, 2009. 1, 2, 3, 5
- [15] E. Elhamifar and R. Vidal. Sparse subspace clustering. In *CVPR*, pages 2790–2797. IEEE, 2009. 1, 2, 3, 4, 5, 7
- [16] E. Elhamifar and R. Vidal. Sparse subspace clustering: Algorithm, theory, and applications. *IEEE Transactions on Pattern Analysis and Machine Intelligence*, 35(11):2765–2781, 2013. 1, 2, 3, 4, 5, 6, 7, 8, 9, 10
- [17] G. Liu, Z. Lin, and Y. Yu. Robust subspace segmentation by low-rank representation. In *ICML*, pages 663–670, 2010. 1, 2, 3, 5, 7
- [18] G. Liu, Z. Lin, S. Yan, J. Sun, Y. Yu, and Y. Ma. Robust recovery of subspace structures by low-rank representation. *IEEE Transactions on Pattern Analysis and Machine Intelligence*, 35(1):171–184, 2013. 1, 2, 3, 5, 7, 8, 9, 10
- [19] Ming Yin, Junbin Gao, Zhouchen Lin, Qinfeng Shi, and Yi Guo. Dual graph regularized latent low-rank representation for subspace clustering. *IEEE Transactions on Image Processing*, 24(12):4918–4933, 2015. 1, 2
- [20] P. Favaro, R. Vidal, and A. Ravichandran. A closed form solution to robust subspace estimation and clustering. In *CVPR*, 2011. 1, 2, 3, 5, 7, 8, 9, 10
- [21] Karavasilis et al. A novel framework for motion segmentation and tracking by clustering incomplete trajectories. *Computer Vision and Image Understanding*, 116(11):11351148, 2012. 1, 2
- [22] Ellis and Ferryman. Biologically-inspired robust motion segmentation using mutual information. *Computer Vision and Image Understanding*, 122:47–64, 2014. 1, 2
- [23] C. Lu, H. Min, Z. Zhao, L. Zhu, D. Huang, and S. Yan. Robust and efficient subspace segmentation via least squares regression. In *ECCV*, pages 347–360. Springer, 2012. 1, 2, 3, 5, 7, 8, 9, 10

- [24] H. Hu, Z. Lin, J. Feng, and J. Zhou. Smooth representation clustering. In *CVPR*, pages 3834–3841, 2014. 1, 2, 3, 5, 7, 9, 10
- [25] X. Peng, L. Zhang, and Z. Yi. Scalable sparse subspace clustering. In *CVPR*, June 2013. 1, 2, 3, 5
- [26] J. Feng, Z. Lin, H. Xu, and S. Yan. Robust subspace segmentation with block-diagonal prior. In *CVPR*, pages 3818–3825, 2014. 1, 2, 3, 5
- [27] B. Li, Y. Zhang, Z. Lin, and H. Lu. Subspace clustering by mixture of gaussian regression. In *CVPR*, pages 2094–2102, 2015. 1, 2, 3, 5
- [28] C. Li and R. Vidal. Structured sparse subspace clustering: A unified optimization framework. In *CVPR*, pages 277–286, 2015. 1, 2, 3, 5, 7, 8, 9
- [29] C. G. Li, C. You, and R. Vidal. Structured sparse subspace clustering: A joint affinity learning and subspace clustering framework. *IEEE Transactions on Image Processing*, 26(6):2988–3001, June 2017. 1, 2, 3, 5, 7, 8, 9, 10
- [30] Jun Xu, Kui Xu, Ke Chen, and Jishou Ruan. Reweighted sparse subspace clustering. *Computer Vision and Image Understanding*, 138(0):25–37, 2015. 1, 2, 3, 5
- [31] C. You, D. Robinson, and R. Vidal. Scalable sparse subspace clustering by orthogonal matching pursuit. In *CVPR*, pages 3918–3927, 2016. 1, 2, 3, 5, 7, 8, 9, 10
- [32] C. Peng, Z. Kang, and Q. Cheng. Subspace clustering via variance regularized ridge regression. In *CVPR*, 2017. 1, 2, 3, 5
- [33] M. Yin, S. Xie, Z. Wu, Y. Zhang, and J. Gao. Subspace clustering via learning an adaptive low-rank graph. *IEEE Transactions on Image Processing*, 27(8):3716–3728, Aug 2018. 1, 2
- [34] Ulrike Von Luxburg. A tutorial on spectral clustering. *Statistics and Computing*, 17(4):395–416, 2007. 1
- [35] D. Lee and H. Seung. Learning the parts of objects by non-negative matrix factorization. *Nature*, 401(6755):788–791, 1999. 1
- [36] S. Boyd, N. Parikh, E. Chu, B. Peleato, and J. Eckstein. Distributed optimization and statistical learning via the alternating direction method of multipliers. *Found. Trends Mach. Learn.*, 3(1):1–122, January 2011. 2, 4, 5, 11, 12
- [37] R. Tron and R. Vidal. A benchmark for the comparison of 3d motion segmentation algorithms. In *CVPR*, 2007. 2, 5, 6, 7, 8, 9, 10
- [38] A.S. Georgiades, P.N. Belhumeur, and D.J. Kriegman. From few to many: Illumination cone models for face recognition under variable lighting and pose. *IEEE Trans. Pattern Anal. Mach. Intelligence*, 23(6):643–660, 2001. 2, 5, 6, 7, 8, 9, 10, 11
- [39] Y. LeCun, L. Bottou, Y. Bengio, and P. Haffner. Gradient-based learning applied to document recognition. *Proceedings of the IEEE*, 86(11):2278–2324, 1998. 2, 5, 6, 7, 8, 9, 10, 11
- [40] E. Candès, J. Romberg, and T. Tao. Robust uncertainty principles: Exact signal reconstruction from highly incomplete frequency information. *IEEE, Trans. Info. Theory*, 52(2):489–509, 2006. 2
- [41] D. Donoho. Compressed sensing. *IEEE, Trans. Info. Theory*, 52(4):1289–1306, 2006. 2
- [42] A. Ng, M. Jordan, and Y. Weiss. On spectral clustering analysis and an algorithm. In *NIPS*, volume 14, pages 849–856, 2001. 2, 5
- [43] J. Shi and J. Malik. Normalized cuts and image segmentation. *IEEE Transactions on Pattern Analysis and Machine Intelligence*, 22(8):888–905, 2000. 3, 5
- [44] R. Courant. Variational methods for the solution of problems of equilibrium and vibrations. *Bull. Amer. Math. Soc.*, 49(1):1–23, 1943. 4, 11, 12
- [45] J. Eckstein and D. P. Bertsekas. On the Douglas–Rachford splitting method and the proximal point algorithm for maximal monotone operators. *Mathematical Programming*, 55(1):293–318, 1992. 4, 11, 12
- [46] J. Nocedal and S. J. Wright. *Numerical Optimization*. Springer, New York, 2nd edition, 2006. 4
- [47] E. Elhamifar, G. Sapiro, and S. Sastry. Dissimilarity-based sparse subset selection. *IEEE Transactions on Pattern Analysis and Machine Intelligence*, 38(11):2182–2197, 2016. 4
- [48] C. Michelot. A finite algorithm for finding the projection of a point onto the canonical simplex of \mathbb{R}^n . *J. Optim. Theory Appl.*, 50(1):195–200, July 1986. 4
- [49] J. Duchi, S. Shalev-Shwartz, Y. Singer, and T. Chandra. Efficient projections onto the ℓ_1 -ball for learning in high dimensions. In *ICML*, pages 272–279. ACM, 2008. 4, 12
- [50] L. Condat. Fast projection onto the simplex and the ℓ_1 ball. *Mathematical Programming*, 158(1):575–585, Jul 2016. 4
- [51] Robert Tibshirani. Regression shrinkage and selection via the lasso. *Journal of the Royal Statistical Society. Series B (Methodological)*, 58(1):267–288, 1996. 5, 6
- [52] I. Jolliffe. Principal component analysis and factor analysis. In *Principal Component Analysis*, pages 115–128. Springer, 1986. 6
- [53] J. Bruna and S. Mallat. Invariant scattering convolution networks. *IEEE Transactions on Pattern Analysis and Machine Intelligence*, 35(8):1872–1886, 2013. 6, 10